Molecular Plant Pathology

MOLECULAR PLANT PATHOLOGY (2019) **20**(2), 194–210 DOI: 10.1111/mpp.12748

Cell death triggered by the P25 protein in *Potato virus X*-associated synergisms results from endoplasmic reticulum stress in *Nicotiana benthamiana*

EMMANUEL AGUILAR[1], FRANCISCO J. DEL TORO[1], CHANTAL BROSSEAU[2], PETER MOFFETT[2], TOMÁS CANTO[1] AND FRANCISCO TENLLADO[1*]

[1]*Departamento de Biotecnología Microbiana y de Plantas, Centro de Investigaciones Biológicas, CSIC, Madrid 28040, Spain*
[2]*Centre SÈVE, Département de Biologie, Université de Sherbrooke, Sherbrooke QC J1K 2R1, Canada*

SUMMARY

The synergistic interaction of *Potato virus X* (PVX) with a number of potyviruses results in systemic necrosis in *Nicotiana* spp. Previous investigations have indicated that the viral suppressor of RNA silencing (VSR) protein P25 of PVX triggers systemic necrosis in PVX-associated synergisms in a threshold-dependent manner. However, little is still known about the cellular processes that lead to this necrosis, and whether the VSR activity of P25 is involved in its elicitation. Here, we show that transient expression of P25 in the presence of VSRs from different viruses, including the helper component-proteinase (HC-Pro) of potyviruses, induces endoplasmic reticulum (ER) stress and the unfolded protein response (UPR), which ultimately lead to ER collapse. However, the host RNA silencing pathway was dispensable for the elicitation of cell death by P25. Confocal microscopy studies in leaf patches co-expressing P25 and HC-Pro showed dramatic alterations in ER membrane structures, which correlated with the up-regulation of bZIP60 and several ER-resident chaperones, including the ER luminal binding protein (BiP). Overexpression of BiP alleviated the cell death induced by the potexviral P25 protein when expressed together with VSRs derived from different viruses. Conversely, silencing of the UPR master regulator, bZIP60, led to an increase in cell death elicited by the P25/HC-Pro combination as well as by PVX-associated synergism. In addition to its role as a negative regulator of P25-induced cell death, UPR partially restricted PVX infection. Thus, systemic necrosis caused by PVX-associated synergistic infections is probably the effect of an unmitigated ER stress following the overaccumulation of a viral protein, P25, with ER remodelling activity.

Keywords: cell death, endoplasmic reticulum, *Potato virus X*, systemic necrosis, unfolded protein response, viral synergism.

*Correspondence: Email: tenllado@cib.csic.es

INTRODUCTION

Positive-strand RNA viruses replicate their genomic RNAs (gRNAs) using host membranous structures, which are extensively remodelled in a process that includes membrane synthesis (den Boon and Ahlquist, 2010). Virus-induced membranous vesicles are derived from different organelles, including the endoplasmic reticulum (ER), to provide a platform for virion assembly, and possibly to shield them from recognition by host defence responses. Such membrane modification is attributable to the action of membrane-targeted viral proteins which, when expressed alone, can induce ER rearrangements similar to those observed in virus-infected cells (Hashimoto *et al.*, 2015; Luan *et al.*, 2016; Tilsner *et al.*, 2012).

The ER is the processing factory for the synthesis and folding of proteins destined for secretion or membrane insertion. Under abiotic and biotic stresses, the accumulation of nascent and unfolded proteins in the lumen of the ER may rapidly exceed its folding capacity, thereby perturbing the normal function of the ER. This can result in ER stress and subsequent triggering of protective signalling pathways, termed the unfolded protein response (UPR) (Bao and Howell, 2017). The role of the UPR is to orchestrate adaptation to ER stress and to restore ER function, prolonging cell viability. Alternatively, under conditions of severe or chronic ER stress, the UPR activates alternative routes, leading to programmed cell death (PCD) (Williams *et al.*, 2014).

The expression of viral proteins, with the associated disruption of normal protein synthesis and cellular balance, can cause ER stress and UPR in plants. Some reported examples include the triple gene block 3 (TGB3) movement protein of *Potato virus X* (PVX) (Ye *et al.*, 2011), the 6K2 membrane binding protein of *Turnip mosaic virus* (TuMV) (Zhang *et al.*, 2015), the P10 outer capsid protein of *Rice black-streak dwarf virus* (RBSDV) (Sun *et al.*, 2013) and the P11 movement protein of *Garlic virus X* (GarVX) (Lu *et al.*, 2016). PVX infection, as well as ectopic expression of PVX TGB3, led to increasing expression of bZIP60 and UPR-related genes, such as ER luminal binding protein (BiP), calreticulin (CRT) and calmodulin (CAM) (Ye *et al.*, 2011). bZIP60

is a downstream transcription factor that activates the genes required for coping with UPR. Remarkably, PVX accumulation was significantly elevated in bZIP60-silenced *Nicotiana benthamiana* plants, suggesting that UPR limits the local accumulation of potexvirus. However, bZIP60 silencing did not induce necrosis in PVX-infected plants (Arias Gaguancela *et al.*, 2016). In addition, the TGB3 protein elicited PCD when expressed either from the *Tobacco mosaic virus* (TMV) genome or from the *Cauliflower mosaic virus* (CaMV) 35S promoter (Ye *et al.*, 2013, 2011).

Systemic necrosis is one of the most severe symptoms caused by plant viruses, which eventually leads to cell death in virus-infected systemic leaves (Syller, 2012). In several compatible pathosystems, systemic necrosis has been shown to share biochemical, physiological and molecular features with the hypersensitive response (HR), a form of PCD (García-Marcos *et al.*, 2013; Komatsu *et al.*, 2010; Mandadi and Scholthof, 2013). Co-infection, but not single infection, of *N. benthamiana* plants with PVX and several members of the *Potyvirus* genus results in systemic necrosis, which correlates with the transcriptional activation of defence-related genes and PCD (García-Marcos *et al.*, 2013, 2009). Contrary to that which has been observed in other PVX-associated synergisms (De *et al.*, 2018; Vance, 1991), the levels of PVX gRNA were not substantially increased in *N. benthamiana* plants when doubly infected with PVX and either *Plum pox virus* (PPV), *Potato virus Y* (PVY) or *Tobacco etch virus*, despite the synergism in pathology that leads to extreme augmentation of symptoms in this host (González-Jara *et al.*, 2005, 2004). We further showed that *Agrobacterium*-mediated transient co-expression of PVX together with viral suppressors of RNA silencing (VSRs) recapitulated in local tissues the systemic necrosis caused by PVX–potyvirus synergistic infections (Aguilar *et al.*, 2015). Moreover, ectopic expression of the potexviral P25 (TGB1) protein encoded by the TGB subgenomic RNA (sgRNA) was sufficient to elicit a cell death response when overexpressed with other VSRs, including the helper component-proteinase (HC-Pro) protein of potyvirus. A frameshift mutation in the P25 open reading frame (ORF) of PVX, which maintained unaltered the TGB3 gene, did not lead to necrosis when co-expressed with VSRs, suggesting that P25 is the main PVX determinant involved in the elicitation of a systemic HR-like response in PVX-associated synergisms.

P25 of potexviruses is a multifunctional protein that acts as a suppressor of RNA silencing by targeting RNA-dependent RNA polymerase6 (RDR6) and Suppressor of Gene Silencing3 (SGS3) (Okano *et al.*, 2014), two key components of the RNA silencing machinery. In addition, it has been shown that P25 directly affects only a subset of the Argonaute (AGO) family of proteins, probably indicating that its suppressor function is mediated by the preclusion of AGO proteins from accessing viral RNA, as well as by direct inhibition of the RNA silencing machinery (Brosseau and Moffett, 2015; Chiu *et al.*, 2010). Previously, it has been reported that the silencing suppression activity of PVX P25 correlates with its capacity to induce cell death in *N. benthamiana* (Aguilar *et al.*, 2015). Moreover, it has been suggested that, as described for other avirulence (avr) determinants with VSR activity (Angel and Schoelz, 2013; Király *et al.*, 1999; Wang *et al.*, 2015), P25 could be recognized as an avr protein that would trigger an HR-like response once it reaches a threshold level by the action of other VSRs. Indeed, P25 elicits a bona fide HR in potato cultivars expressing the *Nb* resistance gene (Malcuit *et al.*, 1999).

In addition to its function as a VSR, P25 is responsible for the extensive rearrangements of actin and endomembranes (ER and Golgi) induced during PVX infection (Tilsner *et al.*, 2012). In several cases, ER membrane reorganization due to the expression of viral proteins is associated with cell death (Hashimoto *et al.*, 2015; Lu *et al.*, 2016). Thus, it is possible that the actin/endomembrane remodelling activities of P25 could be related to its role as an elicitor of cell death. In summary, the mechanism of cell death induction by the P25 protein in the context of PVX-associated synergisms remains unclear, especially in terms of the relationship with the ER rearrangement activity and its function as a suppressor of RNA silencing. In this study, we show that ER membrane modification induced by the PVX P25 protein triggered a UPR when expressed in combination with VSRs. However, despite induction of the UPR, ER stress remained unresolved in leaves expressing either combinations of P25 and VSRs or PVX together with PPV HC-Pro, which ultimately led to cell death. Furthermore, we show that UPR-related mechanisms mediated by BiP and bZIP60 can also limit the multiplication and spread of PVX.

RESULTS

Expression of P25 together with HC-Pro induces the collapse of the ER

The P25 protein of PVX was responsible for the cell death response in PVX-associated synergism (Fig. S1, see Supporting Information; Aguilar *et al.*, 2015). We asked whether ER reorganization mediated by P25 might play a role in the induction of cell death. *Nicotiana benthamiana* leaf patches were infiltrated with *Agrobacterium* cultures expressing β-glucuronidase (GUS), P25 or PPV HC-Pro alone, or a combination of P25 plus HC-Pro. We used transgenic *N. benthamiana* plants that constitutively expressed green fluorescent protein (GFP) targeting the cortical ER (line 16c) (Ruíz *et al.*, 1998). At 6 days post-infiltration (dpi), granular structures associated with disruption of the ER network were observed in the cytoplasm of cells expressing P25 plus HC-Pro (Fig. 1A, bottom right panel), but not in cells expressing P25, HC-Pro or GUS. In addition, large inclusion bodies were evident in patches infiltrated with P25 plus HC-Pro and, to a lesser extent, in patches with P25 alone. Eventually, the ER network fragmented into smaller pieces which led to the collapse of the cells in patches infiltrated with the P25 plus HC-Pro combination at 8 dpi.

To correlate the changes in ER membrane reorganization with cell death, leaf discs from 16c transgenic and wild-type (wt) plants were excised and assayed for electrolyte leakage, a quantitative indicator of cell membrane injury which correlates strongly with cell death (Aguilar *et al.*, 2015). Consistent with the above results, the combination of P25 together with HC-Pro and, to a lesser extent, P25 alone resulted in the strong production of electrolytes indicative of necrosis in 16c and wt plants at 8 dpi (Fig. 1B). We confirmed that HC-Pro and transgene GFP accumulated in 16c patches infiltrated with P25 + HC-Pro at levels comparable with patches infiltrated with either HC-Pro or P25 alone (Fig. 1C). The higher levels of P25 accumulation observed in the combination of P25 with HC-Pro compared with P25 alone is probably a result of the stronger silencing suppression activity of HC-Pro compared with that of P25 (Senshu *et al.*, 2009).

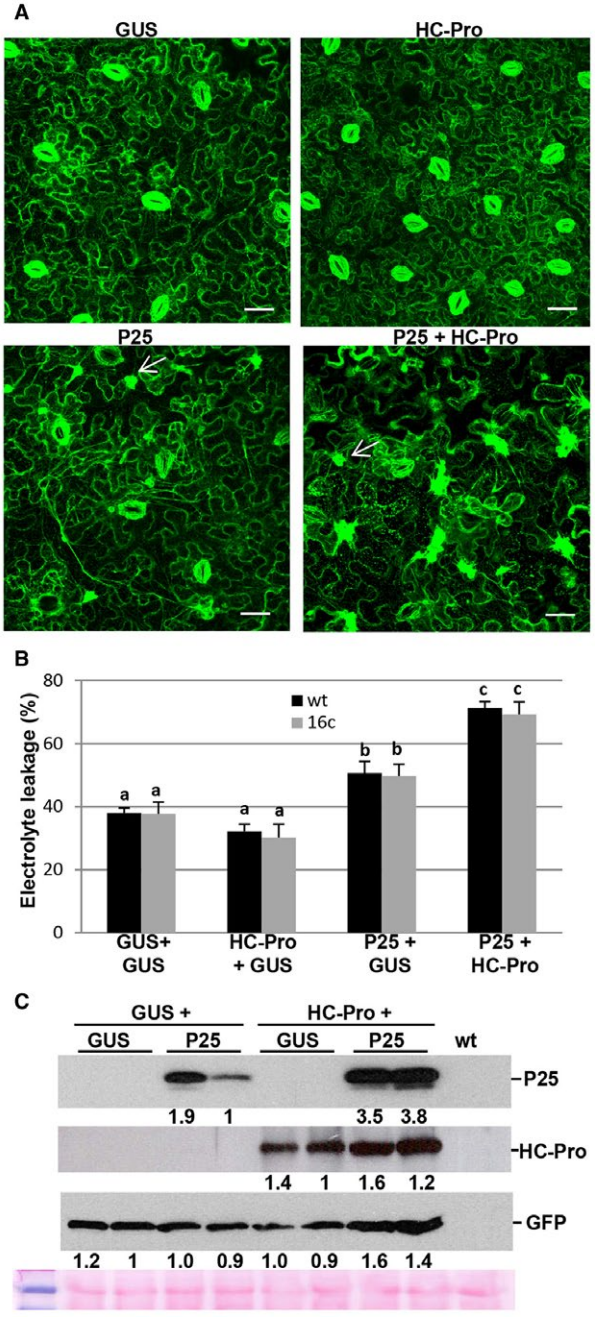

Fig. 1 Visualization of endoplasmic reticulum (ER) modification in cells co-expressing *Potato virus X* (PVX) P25 together with *Plum pox virus* (PPV) helper component-proteinase (HC-Pro). (A) Transgenic *Nicotiana benthamiana* plants expressing ER-GFP (line 16c) were infiltrated with *Agrobacterium* cultures expressing P25, HC-Pro or β-glucuronidase (GUS) alone or a combination of cultures expressing P25 plus HC-Pro, as indicated. Granular structures associated with disruption of the ER network were visible in cells expressing P25 plus HC-Pro (bottom right panel), but not in cells expressing P25, HC-Pro or GUS. Large irregular inclusions (arrows) were also evident in patches infiltrated with P25 plus HC-Pro and, to a minor extent, in patches with P25 alone. Photographs were taken at 6 days post-infiltration (dpi). Bars in each panel represent 45 μm. (B) 16c and wild-type (wt) *N. benthamiana* leaves were infiltrated with *Agrobacterium* cultures expressing T7-tagged P25, HC-Pro or green fluorescent protein (GFP) alone, or a combination of cultures expressing T7-tagged P25 plus HC-Pro. Leaf discs were excised and assayed for electrolyte leakage at 8 dpi. Data represent the means ± standard errors of five replicates, each consisting of four plants that received the same treatment. Statistically significant differences between means were determined by employing Scheffé's multiple range test for between-group comparisons. Different letters indicate significant differences at $P < 0.05$. (C) Western blot analyses of extracts derived from 16c leaf patches at 8 dpi, using antibodies against the T7 epitope (top panel), PPV HC-Pro (middle panel) or GFP (bottom panel). The lowest panel below the western blots shows the Ponceau S-stained membrane after blotting, as a loading control. The intensities of the P25, HC-Pro and GFP bands, normalized for the loading controls, were quantified by densitometric analyses. [Colour figure can be viewed at wileyonlinelibrary.com]

Modification of ER membranes is often associated with *de novo* membrane synthesis. We investigated whether cell death induced by the P25 protein was influenced by cerulenin, an inhibitor of *de novo* lipid synthesis (Omura, 1976). For this purpose, cerulenin (200 μM) or dimethyl sulfoxide (DMSO) as a control was infiltrated into wt *N. benthamiana* leaves in combination with *Agrobacterium* expressing GUS, P25 or HC-Pro alone, or a combination of P25 plus HC-Pro. When the combination P25 plus HC-Pro or P25 alone was co-infiltrated with cerulenin, the level of electrolyte leakage was significantly lower than that in the controls at 8 dpi (Fig. 2A). Consistent with this finding, the production of hydrogen peroxide (H_2O_2), indicative of cell death, was attenuated in patches infiltrated with P25 plus HC-Pro (Fig. 2B), although the expression of P25 was not influenced by cerulenin treatment (Fig. 2C). When P25 and HC-Pro were co-infiltrated with cerulenin in 16c transgenic leaves, granular structures associated with disruption of the ER were clearly inhibited at 6 dpi compared with untreated P25 + HC-Pro-expressing leaves (Fig. 2D). These results suggest that P25-induced ER modification could result in the induction of cell death, and that this process requires continuous lipid biosynthesis.

Previous studies have revealed that the ER network and its mobility are associated with the actin cytoskeleton (Sparkes *et al.*, 2009). As it has been shown that PVX P25 remodels host actin and endomembranes (Tilsner *et al.*, 2012), we used the microfilament inhibitor latrunculin B (LatB) to examine the influence of actin organization on P25-induced cell death. Wt *N. benthamiana* leaves were treated with LatB (10 μM) or DMSO 4 days after infiltration with HC-Pro plus either GUS or P25. No statistical differences in electrolyte leakage were observed between LatB-treated patches and controls (Fig. 2E), suggesting that an intact actin cytoskeleton is not required for P25-induced cell death.

Cell death induced by P25/HC-Pro does not rely on RNA silencing mechanisms

Previously, it has been reported that the silencing suppression activity of P25 correlates with the cell death response (Aguilar *et al.*, 2015). To evaluate whether the RNA silencing suppressor activity of P25 is required for the induction of ER membrane reorganization, three single amino acid mutants of P25, A104V, T117A and K124E, reported previously, were used for analysis (Aguilar *et al.*, 2015). 16c transgenic plants were infiltrated with *Agrobacterium* cultures expressing GUS, P25wt or HC-Pro alone or combinations of HC-Pro plus either P25wt or P25 mutants. The combination of HC-Pro together with the silencing suppression-competent P25 mutant A104V led to disruption of the ER network at 8 dpi, similar to that observed in P25wt + HC-Pro-infiltrated areas (Fig. 3A). Remarkably, leaf patches infiltrated with HC-Pro plus the silencing suppression-deficient mutants T117A or K124E did not undergo drastic rearrangement of the ER network structure compared with patches infiltrated with P25wt or P25 mutant A104V. We confirmed that P25 mutants A104V, T117A and K124E accumulated in the infiltrated patches at comparable levels to P25wt, as assayed by western blot analysis (Fig. 3B). These observations, together with previously reported data showing that T117A and K124E, but not A104V, abolished the capacity of P25 protein to elicit cell death (Aguilar *et al.*, 2015), suggest that the capacity of the P25 protein to disrupt ER membrane structures could be linked to its suppressor activity, or at least that it maps to the same protein domain responsible for VSR activity.

To study the contribution, if any, of RNA silencing to the cell death response elicited by P25, several genetic approaches were undertaken. First, we used *N. benthamiana* transgenic lines suppressed for each one of the four known Dicer-like (DCLi) genes and for a combination of DCL2 and DCL4 (DCL2/4i). DCL genes are core components of host RNA-mediated silencing pathways. Quantitative reverse transcription-polymerase chain reaction (qRT-PCR) and semi-quantitative RT-PCR analyses of transgenic lines DCL1i, DCL2i, DCL3i and DCL4i have shown previously a specific reduction in DCL1, DCL2, DCL3 and DCL4 mRNA levels, respectively (Dadami *et al.*, 2013). We agroinfiltrated wt and DCL1i, DCL2i, DCL3i, DCL4i and DCL2/4i lines with *Agrobacterium* cultures expressing GUS, P25 or HC-Pro alone, or a combination of P25 plus HC-Pro, and assayed for electrolyte leakage. There were no statistical differences in electrolyte leakage between DCL1i, DCL2i, DCL3i, DCL4i and DCL2/4i lines compared with wt in patches infiltrated with P25 + HC-Pro at 8 dpi (Fig. 4A).

P25 of potexviruses has been reported to target components in the antiviral RNA silencing pathway, such as RDR6 and SGS3 (Okano *et al.*, 2014). Transgenic hairpin-mediated silencing of RDR6 (RDR6i line) and virus-induced gene silencing (VIGS) of SGS3 (Fig. S2, see Supporting Information) did not alter the cell death induced by the co-expression of P25 together with HC-Pro, as assayed by electrolyte leakage (Fig. 4C,E).

Next, we undertook a different approach by transiently overexpressing AGO proteins together with P25 or HC-Pro alone, or a combination of HC-Pro plus P25, in wt *N. benthamiana* leaves. This included *N. benthamiana* AGO2 and AGO4, as well as Arabidopsis AGO2, which has been reported to interact with P25 (Chiu *et al.*, 2010). Within each group of plants, no statistical differences in electrolyte leakage were observed between AGO-overexpressing patches and controls (Fig. 4G). The overexpression of the different AGO proteins was confirmed by RT-PCR (Fig. S2). In all of these assays with overexpressing/silencing-deficient plants, we confirmed that P25 accumulated at greater levels in patches infiltrated with P25 plus HC-Pro than in patches infiltrated with P25 alone, i.e. an increase comparable with that shown by wt and control plants (Fig. 4,B,D,F,H). Altogether, these findings suggest that there is not a causal relationship between the suppression of RNA silencing and the cell death response elicited by the P25/HC-Pro combination.

The UPR is induced by P25/HC-Pro co-expression

It has been reported that certain viral proteins can cause ER stress and UPR in plants. We tested whether ER membrane reorganization due to co-expression of P25 together with HC-Pro was associated with UPR. Wt *N. benthamiana* leaves were infiltrated with each binary construct alone or with the combination of P25 together with HC-Pro. We next examined the mRNA levels of genes associated with UPR, including those encoding bZIP60 and ER-resident chaperones, such as BiP, heat shock protein 90-2 (HSP90-2), S-phase kinase-associated protein 1 (SKP1), CRT and CAM. bZIP60 is known to up-regulate BiP as part of an ER stress response (Bao and Howell, 2017). BiP and HSP90-2 are chaperones that restore proper protein folding during ER stress. SKP1 is a component of the SCF-type E3 ubiquitin ligase complex that is implicated in the elimination of misfolded proteins. CRT is a lectin that recognizes N-linked oligosaccharides on glycoproteins. CAM is a Ca^{2+} sensor that activates immune-related PCD. qRT-PCR analysis showed that BiP, bZIP60, HSP90-2, SKP1 and CRT

were significantly induced in leaf patches expressing P25 plus HC-Pro compared with patches expressing GFP, HC-Pro or P25 alone at 3 dpi. Transcript levels of CAM were found to be induced in patches expressing P25 plus HC-Pro at 6 dpi (Fig. 5). These observations suggest that the combination of P25 plus HC-Pro induces ER stress and the UPR in *N. benthamiana*.

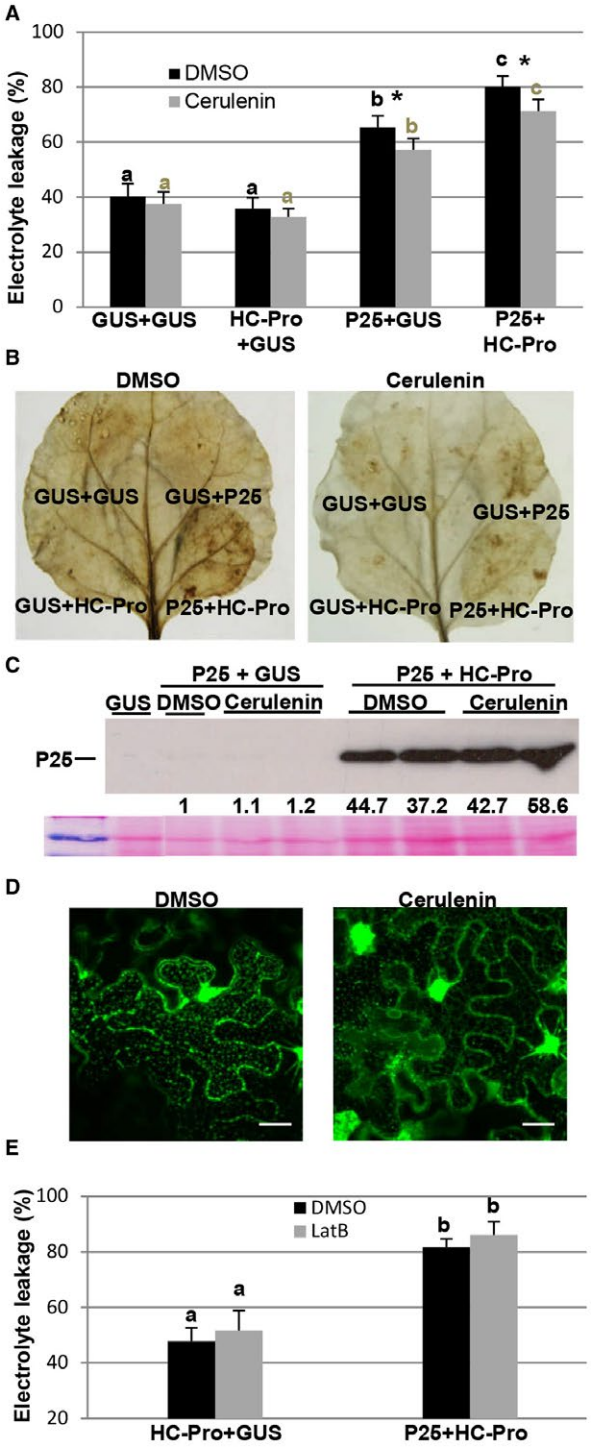

Fig. 2 Effect of cerulenin treatment on the cell death response induced by P25/helper component-proteinase (HC-Pro). (A) Wild-type (wt) *Nicotiana benthamiana* leaves were infiltrated with *Agrobacterium* cultures expressing T7-tagged P25, HC-Pro or green fluorescent protein (GFP) alone, or a combination of cultures expressing T7-tagged P25 plus HC-Pro, in combination with cerulenin (200 μM) or dimethyl sulfoxide (DMSO) as a control. Leaf discs were excised and assayed for electrolyte leakage at 8 days post-infiltration (dpi). (B) Leaves were stained with 3,3′-diaminobenzidine (DAB) solution at 8 dpi. (C) Western blot analysis of extracts derived from leaf patches at 8 dpi, using antibodies against the T7 epitope. The bottom panel below the western blot shows the Ponceau S-stained membrane after blotting, as a loading control. The intensity of the P25 bands, normalized for the loading controls, was quantified by densitometric analysis. The value for the band in leaf patches infiltrated with P25-T7 plus β-glucuronidase (GUS) (DMSO) was set at unity and the other data were calculated relative to this value. (D) Effect of cerulenin treatment on P25 + HC-Pro-induced membrane modification in transgenic *N. benthamiana* plants expressing endoplasmic reticulum (ER)-GFP (line 16c). Photographs were taken at 6 dpi. The bars in each panel represent 20 μm. (E) Wt *N. benthamiana* leaves were infiltrated with either latrunculin B (LatB, 10 μM) or a DMSO buffer control at 4 days after infiltration with combinations of *Agrobacterium* cultures expressing HC-Pro plus either GUS or P25. Leaf discs were excised and assayed for electrolyte leakage at 8 dpi. Data represent the means ± standard errors of six replicates, each consisting of four plants that received the same treatment. Statistically significant differences between means were determined by employing Scheffé's multiple range test for between-group comparisons. Different letters indicate significant differences at $P < 0.05$. For pairwise comparisons, asterisks indicate significant differences between treatments (Student's *t*-test, $P < 0.05$). [Colour figure can be viewed at wileyonlinelibrary.com]

The UPR attenuates the cell death response elicited by P25/HC-Pro

It has been reported that overexpression of the PVX TGB3 protein leads to ER stress-related cell death in *N. benthamiana*, which can be alleviated by the ER-resident chaperone BiP (Ye *et al.*, 2011). To determine whether P25-mediated necrosis could be alleviated by BiP, leaf patches were infiltrated with a mixture of *Agrobacterium* expressing P25 and HC-Pro in combination with either BiP or GFP. Overexpression of BiP alleviated cell death and H_2O_2 production elicited by the P25/HC-Pro combination compared with controls at 8 dpi (Fig. 6A,B). We confirmed that P25 accumulated in BiP-overexpressing patches at levels comparable with controls, as assayed by western blot analysis (Fig. 6C). BiP was also detected serologically by western blot in the corresponding patches (Fig. 6C, bottom). To investigate whether the alleviation of P25/HC-Pro-induced cell death by BiP is related to ER membrane modification, P25 plus HC-Pro was co-infiltrated with BiP or GUS in 16c transgenic leaves. Granular structures associated with disruption of the ER were clearly inhibited in leaves expressing P25 + HC-Pro + BiP compared with control leaves at 6 dpi (Fig. 6D).

To determine whether BiP affects the cell death induced by P25 when overexpressed with other VSR proteins, *N. benthamiana* leaf patches were infiltrated with *Agrobacterium* mixtures expressing P25 plus *Tomato bushy stunt virus* (TBSV) P19,

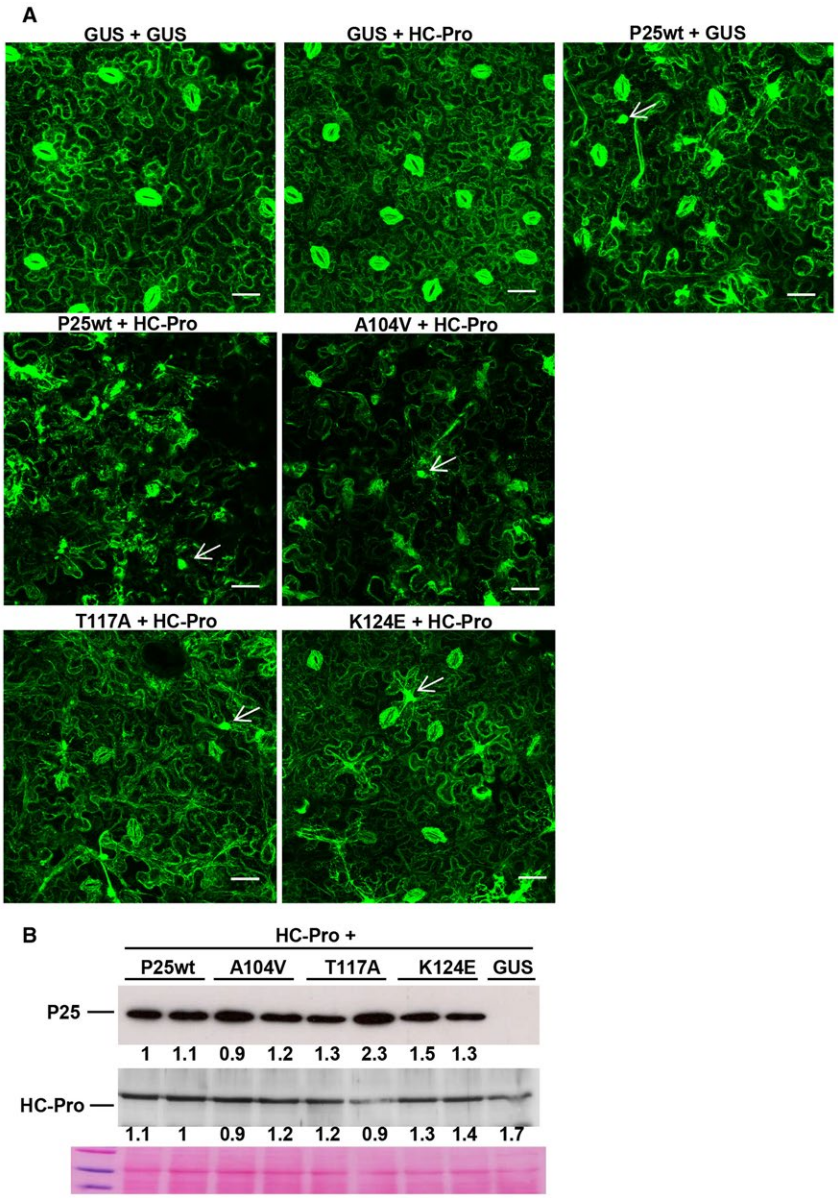

Fig. 3 Disruption of endoplasmic reticulum (ER) correlates with the silencing suppression activity of P25. (A) Transgenic *Nicotiana benthamiana* plants expressing ER-GFP (green fluorescent protein) (line 16c) were infiltrated with *Agrobacterium* cultures expressing T7-tagged P25, helper component-proteinase (HC-Pro) or β-glucuronidase (GUS) alone or a combination of cultures expressing HC-Pro plus T7-tagged versions of either P25wt or P25 A104V, T117A, K124E mutants, as indicated. Large irregular inclusions are marked by arrows. Photographs were taken at 8 days post-infiltration. Bars in each panel represent 45 μm. (B) Western blot analyses of extracts derived from leaf patches at 8 dpi, using antibodies against the T7 epitope (top panel) or *Plum pox virus* (PPV) HC-Pro (middle panel). The lower panel below the western blots shows the Ponceau S-stained membrane after blotting, as a loading control. The intensities of the P25 and HC-Pro bands, normalized for the loading controls, were quantified by densitometric analyses. [Colour figure can be viewed at wileyonlinelibrary.com]

Cucumber mosaic virus (CMV) 2b or *Citrus tristeza virus* (CTV) P23, in combination with either BiP or GFP. The combinations of P25 together with P19, 2b and P23 resulted in the strong production of H_2O_2, indicative of necrosis at 8 dpi, which was alleviated by BiP expression (Fig. S3, see Supporting Information). Further, a reduced cell death response compared with controls was observed when the combination of HC-Pro plus the P25 protein of another potexvirus, *Plantago asiatica mosaic virus* (PlAMV), was expressed together with BiP. However, expression of the combinations of PPV HC-Pro together with TBSV P19 or CMV 2b did not lead to necrosis.

To examine the role of bZIP60 in the cell death response elicited by P25/HC-Pro, we knocked down the expression of bZIP60 by VIGS. *Nicotiana benthamiana* plants were infiltrated with the

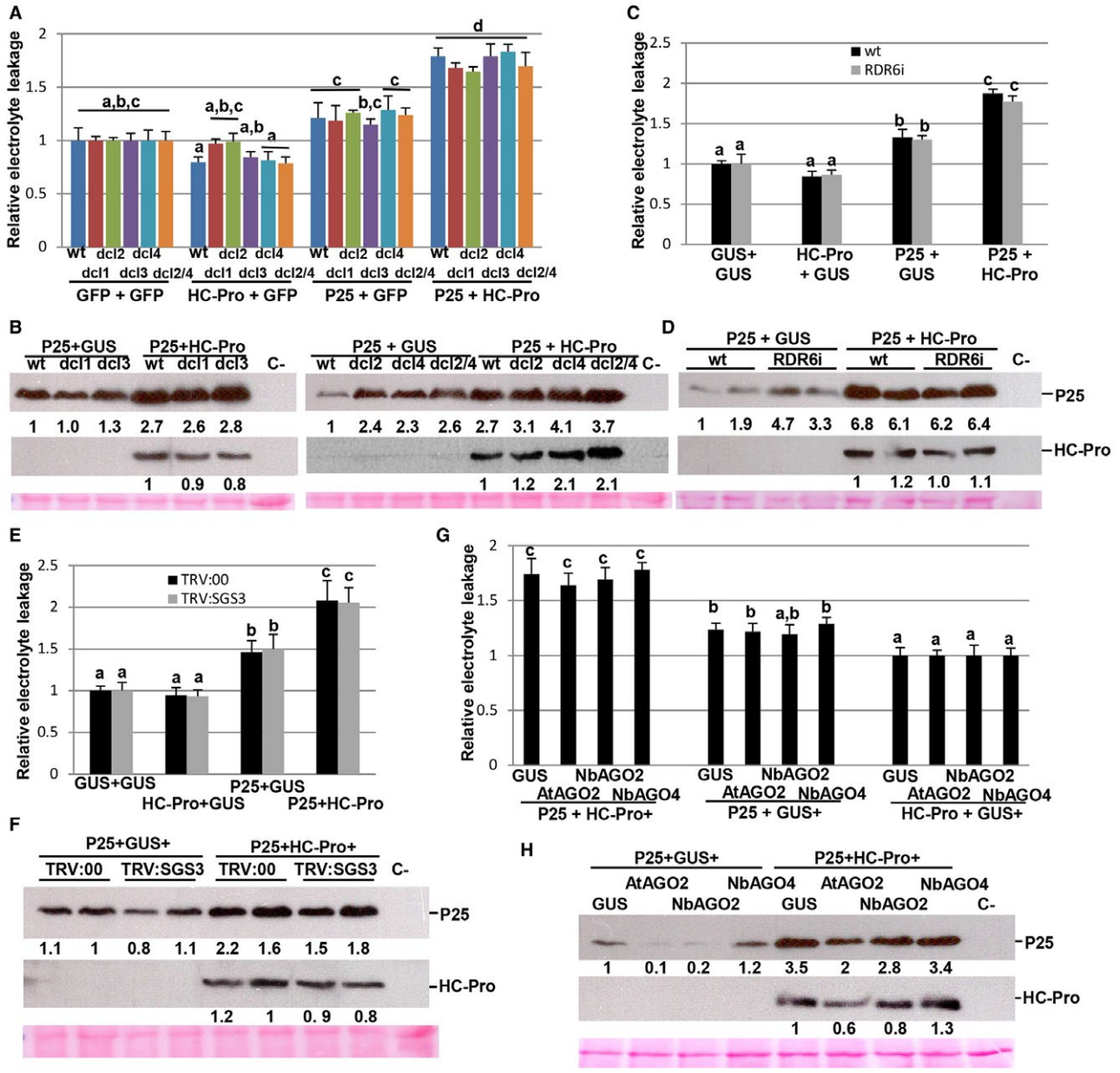

Fig. 4 Different RNA silencing pathways do not alter the cell death response induced by P25/helper component-proteinase (HC-Pro). (A) *Nicotiana benthamiana* transgenic lines suppressed for each one of the four known Dicer-like (DCL) genes and for a combination of DCL2 and DCL4 (DCL2/4) were infiltrated with a combination of *Agrobacterium* cultures expressing T7-tagged P25, HC-Pro or green fluorescent protein (GFP) alone, or a combination of cultures expressing T7-tagged P25 plus HC-Pro. (C) *Nicotiana benthamiana* transgenic lines suppressed for RNA-dependent RNA polymerase6 (RDR6i) were infiltrated with a combination of *Agrobacterium* cultures expressing T7-tagged P25, HC-Pro or β-glucuronidase (GUS) alone, or a combination of cultures expressing T7-tagged P25 plus HC-Pro. (E) Leaves from Suppressor of Gene Silencing3 (SGS3)-silenced (TRV:SGS3) and control (TRV:00) plants were infiltrated with a combination of *Agrobacterium* cultures expressing T7-tagged P25, HC-Pro or GUS alone, or a combination of cultures expressing T7-tagged P25 plus HC-Pro. (G) Wild-type (wt) *N. benthamiana* plants were infiltrated with combinations of *Agrobacterium* cultures expressing *N. benthamiana* Argonaute2 (AGO2) (NbAGO2), AGO4 (NbAGO4), Arabidopsis AGO2 (AtAGO2) or GUS together with HC-Pro or T7-tagged P25 alone, or the combination of HC-Pro plus T7-tagged P25, as indicated. Leaf discs were excised and assayed for electrolyte leakage at 8 days post-infiltration (dpi). The value of control samples was set at unity and the other data were calculated relative to this value. Data represent the means ± standard errors of six replicates, each consisting of four plants that received the same treatment. Statistically significant differences between means were determined by employing Scheffé's multiple range test. Different letters indicate significant differences at $P < 0.05$. (B, D, F, H) Western blot analyses of extracts derived from leaf patches at 8 dpi, using antibodies against the T7 epitope (top panel) or *Plum pox virus* (PPV) HC-Pro (middle panel). The lower panel below the western blots shows the Ponceau S-stained membrane after blotting, as a loading control. The intensities of the P25 and HC-Pro bands, normalized for the loading controls, were quantified by densitometric analyses. [Colour figure can be viewed at wileyonlinelibrary.com]

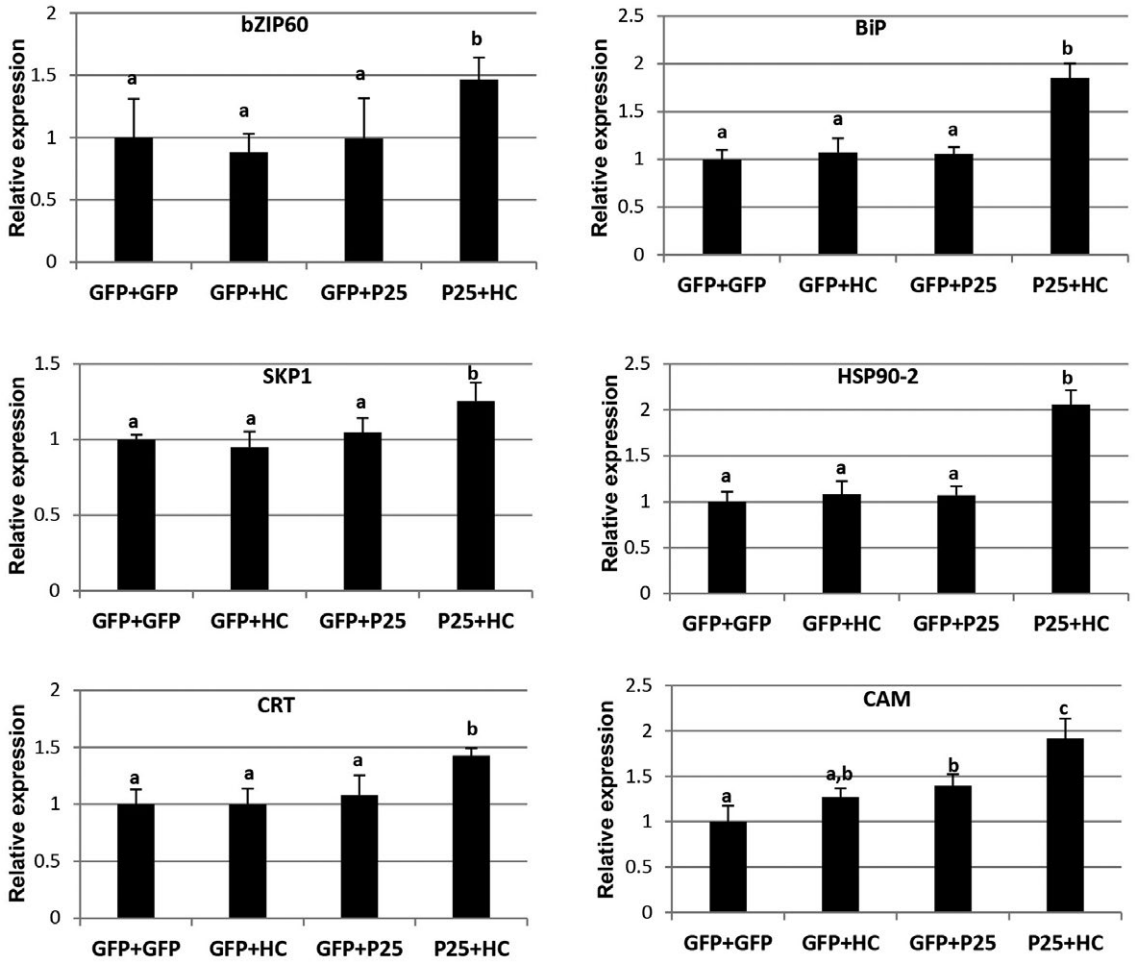

Fig. 5 Co-expression of *Potato virus X* (PVX) P25 together with *Plum pox virus* (PPV) helper component-proteinase (HC-Pro) promotes endoplasmic reticulum (ER) stress. *Nicotiana benthamiana* leaves were infiltrated with *Agrobacterium* cultures expressing T7-tagged P25, HC-Pro or green fluorescent protein (GFP) alone or a combination of cultures expressing T7-tagged P25 plus HC-Pro. Quantitative reverse transcription-polymerase chain reaction (qRT-PCR) analysis of the expression of ER stress marker genes in *N. benthamiana* leaves at 3 [luminal binding protein (BiP), bZIP60, heat shock protein 90-2 (HSP90-2), S-phase kinase-associated protein 1 (SKP1) and calreticulin (CRT)] or 6 days post-infiltration (calmodulin, CAM), as indicated. Expression of the 18S rRNA gene served as a control. Data represent the means ± standard errors of three replicates, each consisting of three plants that received the same treatment. Statistically significant differences between means were determined by employing Scheffé's multiple range test, except for CAM, where these differences were determined by T3 Dunnett's test. Different letters indicate significant differences at $P < 0.05$.

Tobacco rattle virus (TRV) recombinant vector (TRV2:bZIP60) or the empty vector (TRV2:00) as a control. At 20 days after infection, RT-PCR analysis using RNA extracted from the upper leaves confirmed that bZIP60 transcript levels were reduced substantially in bZIP60-silenced plants compared with control plants (Fig. 7A). Combinations of P25 together with HC-Pro or GFP alone as a control were infiltrated in opposite leaf patches of plants silenced for bZIP60 or control plants. The bZIP60-silenced plants infiltrated with P25 plus HC-Pro exhibited significantly higher levels of electrolyte leakage than the control plants at 8 dpi (Fig. 7B). Consistent with the above results, the production of H_2O_2 was enhanced in bZIP60-silenced plants compared with control plants (Fig. 7C). We confirmed that P25 accumulated in bZIP60-silenced plants at levels comparable with those of control plants, as assayed by western blot analysis (Fig. 7D). Altogether, these results demonstrate that bZIP60 and BiP, and therefore the UPR pathway, attenuate the cell death response elicited by P25/VSR combinations.

The UPR attenuates PVX-associated synergism and reduces the local accumulation and systemic spread of PVX

To evaluate whether UPR contributes to ameliorate the cell death induced by PVX-associated synergisms, binary constructs expressing either BiP or GUS were agroinfiltrated together with PVX in the presence or absence of HC-Pro. By 8 dpi,

electrolyte leakage measurement revealed that cell death in BiP-overexpressing patches infiltrated with PVX plus HC-Pro was attenuated compared with that in control patches (Fig. 8A). Consequently, the presence of BiP alleviated the strong necrosis response elicited by PVX in combination with HC-Pro (Fig. 8B). To examine the effect of BiP overexpression on the accumulation level of PVX, we measured the amount of virus in leaf patches from BiP-overexpressing and control samples at 4 and 7 dpi. Comparative analysis by qRT-PCR revealed that the level of PVX gRNA in BiP-overexpressing patches, in the presence or absence of HC-Pro, was lower than that in the controls at 7 dpi, as well as at 4 dpi in the absence of HC-Pro (Fig. 8C). Despite the drastic increase in electrolyte leakage, no significant enhancement in PVX gRNA levels was observed in control plants inoculated with PVX plus HC-Pro relative to plants challenged with PVX alone, supporting the previous findings showing that cell death was not determined by the level of PVX gRNA itself, but by the sgRNA encoding P25 (Aguilar *et al.*, 2015). Similar qRT-PCR results were obtained in an independent experiment when samples were taken at 3 and 6 dpi (Fig. S4, see Supporting Information).

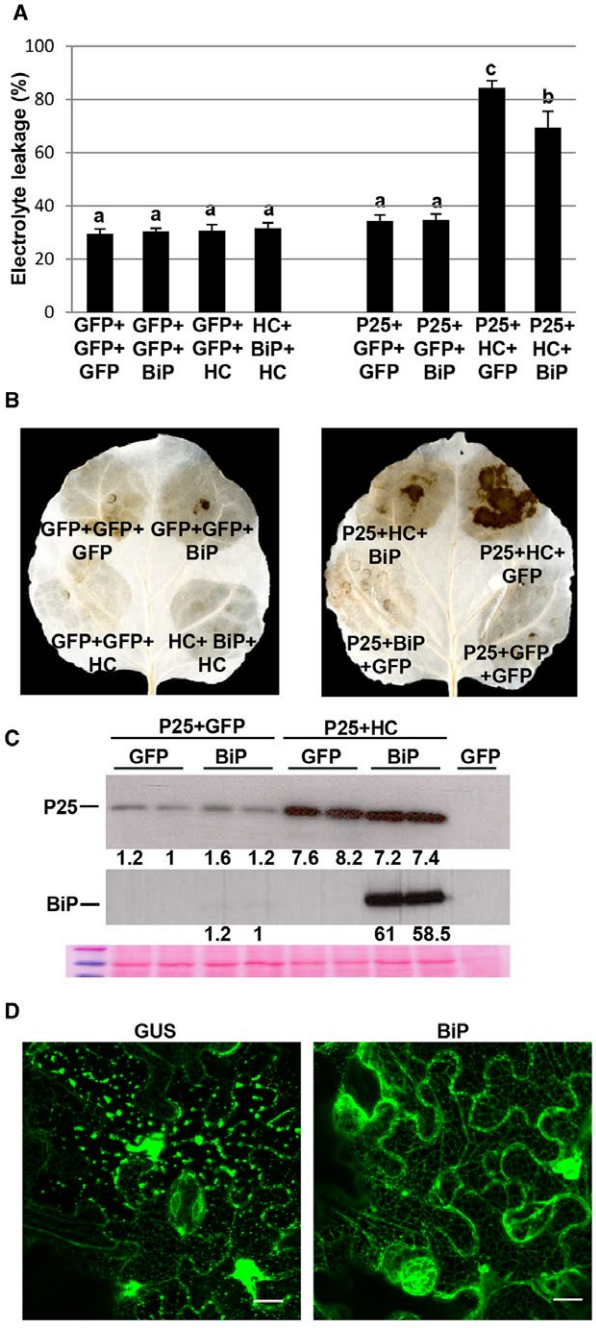

Fig. 6 The overexpression of luminal binding protein (BiP) attenuates the cell death induced by P25/helper component-proteinase (HC-Pro). (A) *Nicotiana benthamiana* leaves were infiltrated with combinations of *Agrobacterium* cultures expressing T7-tagged P25, HC-Pro, BiP or green fluorescent protein (GFP), as indicated. Leaf discs were excised and assayed for electrolyte leakage at 8 days post-infiltration (dpi). Data represent the means ± standard errors of six replicates, each consisting of four plants that received the same treatment. Statistically significant differences between means were determined by employing Scheffé's multiple range test. Different letters indicate significant differences at $P < 0.05$. (B) Leaves were stained with 3,3′-diaminobenzidine (DAB) solution at 8 dpi. (C) Western blot analyses of extracts derived from leaf patches at 8 dpi, using antibodies against the T7 (top panel) or haemagglutinin (middle panel) epitope. The lower panel below the western blots shows the Ponceau S-stained membrane after blotting, as a loading control. The intensities of the P25 and BiP bands, normalized for the loading controls, were quantified by densitometric analyses. (D) Effect of BiP expression on P25 + HC-Pro-induced membrane modification in transgenic *N. benthamiana* plants expressing endoplasmic reticulum (ER)-GFP (line 16c). GUS, β-glucuronidase. Photographs were taken at 6 dpi. Bars in each panel represent 20 μm. [Colour figure can be viewed at wileyonlinelibrary.com]

In a second assay, bZIP60-silenced and control plants were agroinfiltrated with PVX in the presence or absence of HC-Pro. The bZIP60-silenced plants infiltrated with PVX plus HC-Pro exhibited significantly higher levels of electrolyte leakage and necrosis response than did non-silenced control plants at 8 dpi (Fig. 9A,B). PVX gRNA accumulated at higher levels in bZIP60-silenced patches infiltrated with PVX plus HC-Pro compared with control patches, but not in those challenged with PVX alone at 4 and 7 dpi (Fig. 9C).

To further characterize the requirement of UPR for the antiviral defence response, we challenged bZIP60-silenced and control plants with PVX expressing GFP and followed the accumulation of PVX-GFP in systemic tissues. Both the visual intensity of fluorescence and the amounts of GFP detected by western blot showed a higher accumulation of PVX in bZIP60-silenced plants compared with controls at 8 dpi (Fig. 9D,E).

DISCUSSION

The UPR represents a cellular response to ER stress aiming to restore protein homeostasis. Failure of this restoration ultimately leads to the induction of PCD by mechanisms still poorly understood (Bao and Howell, 2017; Williams *et al.*, 2014). In this work,

we focus our attention on the elicitation of UPR and cell death in PVX-associated synergisms.

ER-GFP-transgenic *N. benthamiana* plants and inhibitor assays using cerulenin demonstrated that the P25-induced cell death correlated with dramatic alterations in the cortical ER reticular structure. The granular structures and large inclusion bodies induced by the expression of P25 together with HC-Pro were similar to those induced by the helicase protein encoded by *Radish mosaic virus*, which triggered cell death when overexpressed in *N. benthamiana* (Hashimoto *et al.*, 2015). Previous studies have shown that PVX P25 mutants that have impaired ability to suppress RNA silencing do not induce cell death when synergized by the presence of other VSRs (Aguilar *et al.*, 2015). In this work, two silencing suppression-deficient mutants of P25, T117A and K124E, showed reduced ER membrane modification effects compared with P25wt, suggesting that these mutations affect the conformational structure of the protein that regulates the membrane modification activity. On the other hand, the suppression-competent P25 mutant A104V fully retained its ER membrane modification activity. Such correlation of cell death-inducing activity in the P25 protein with its silencing suppression activity suggests a causal relationship between these two properties. Because the P25-induced cell death has characteristics similar to HR, i.e. strong oxidative stress and degradation of nuclear DNA, amongst others (García-Marcos *et al.*, 2013), it has been suggested that P25 induces cell death mediated by R-like protein recognition once P25 reaches a threshold level by the action of VSRs (Aguilar *et al.*, 2015). Indeed, several studies have shown that a number of viral suppressors of RNA silencing can also act as avr determinants (Angel and Schoelz, 2013; Király *et al.*, 1999; de Ronde *et al.*, 2014), some of which require VSR activity to induce an HR (Chen *et al.*, 2008; Li *et al.*, 1999; Wang *et al.*, 2015). In support of this hypothesis, silencing of SGT1 and RAR1, which are known to play essential roles in many *R*-gene-triggered resistance responses against viruses, reduced both P25-mediated necrosis and systemic necrosis induced by PVX/PPV synergism (Aguilar *et al.*, 2015). Although the hypothetical *R* gene in *N. benthamiana* has not been identified, P25 elicits an HR in potato cultivars expressing the *Nb* gene (Malcuit *et al.*, 1999). Transient expression of a P25-GFP fusion protein in *Nb* potato cells led to the formation of large inclusion bodies, followed by degradation of subcellular structures, similar to those induced by the expression of P25/VSR in *N. benthamiana*.

One of the most commonly accepted models for R–avr recognition is the guard hypothesis, in which the pathogen avr protein targets a host protein under surveillance of the R protein rather than binding directly to the R protein (Moffett, 2016). The guard hypothesis predicts that pathogen perception is achieved by monitoring proteins (guardees) commonly targeted by avr proteins. Thus, we hypothesized that the alteration of the normal levels of the guardee could have an effect on R–P25 recognition, as has been described in Arabidopsis, where the reduction in RIN4 (guardee) via antisense RNA inhibited both the HR and the restriction of *Pseudomonas syringae* growth controlled by the RPM1 resistance protein (Mackey *et al.*, 2002). Here, we tested this hypothesis by the co-expression of P25 in combination with HC-Pro in plants with altered expression of key components of the RNA silencing machinery, several of which have been reported to be targeted by P25 (Brosseau and Moffett, 2015; Chiu *et al.*, 2010; Okano *et al.*, 2014). However, the knockdown of RDR6, SGS3 and Dicer-like genes, as well as the overexpression of NbAGO2, NbAGO4 and AtAGO2, failed to alter the cell death response elicited by the P25/HC-Pro combination, suggesting that none of these proteins are candidates for P25 targeting for indirect detection by the hypothetical *R* gene. Although we cannot rule out that the *N. benthamiana* R protein might recognize directly a suppression-competent conformation of P25, the low sequence identity amongst the P25 proteins from PVX and PlAMV (36%), both of which elicited cell death when synergized with HC-Pro, makes this possibility unlikely. It has been reported that the avr determinant in the potexvirus–*Rx* pathosystem requires a high level of identity amongst the coat proteins of the various recognized viruses (Baurès *et al.*, 2008).

Alternatively, the RNA silencing suppressor activity and induction of cell death by P25 might not be linked by a causal relationship, but may still rely on a structural feature of the protein that is required for both activities. In this scenario, the P25-triggered necrosis may be connected to an essential function of P25 during potexvirus infection. It has been reported that P25 in the absence of other viral factors induces the rearrangement of ER membranes into the so-called X-body, a virally induced inclusion structure that supports PVX replication (Tilsner *et al.*, 2012). In this study, we showed that ER chaperones and protein-folding genes, such as BiP, HSP90-2, SKP1, CRT and CAM, and a transcription factor that is induced during ER stress, bZIP60, were all up-regulated in *N. benthamiana* leaves expressing P25 together with HC-Pro. Although the up-regulation of UPR-related gene expression was somewhat modest in P25/HC-Pro-infiltrated patches, similar increases in these genes (*c.* twofold) were reported in plants systemically infected with the synergistic pair PVX–PVY (García-Marcos *et al.*, 2009). Thus, the extensive rearrangement of ER membranes with the progressive formation of granular structures and large inclusion bodies during the ectopic expression of P25 probably disturbs ER homeostasis and causes ER stress. However, despite the induction of UPR, stress on the ER remained unresolved in P25/VSR-infiltrated patches, which ultimately led to cell death. It should be noted that UPR-related gene expression was an early response to the ectopic expression of P25/HC-Pro that preceded the onset of cell death, as has been reported in other examples of ER-targeted viral proteins that lead to cell death (Lu *et al.*, 2016; Ye *et al.*, 2013, 2011). Similarly, we propose that co-infections of PVX with other viruses expressing

strong VSRs could mimic HC-Pro action on P25, allowing P25 to accumulate to very high levels with a detrimental effect on ER homeostasis, subsequently leading to necrosis in systemic leaves. The expression of P25 from the PVX genome is tightly regulated by the low levels of expression of the TGB sgRNA (Verchot *et al.*, 1998), suggesting that the control of P25 expression might represent a strategy of the virus to avoid detrimental effects in the host. It has been shown that the accumulation of PVX sgRNA encoding P25, but not gRNA, increases in plants doubly infected with PVX and PPV, and by the co-expression of PVX together with PPV HC-Pro (Aguilar *et al.*, 2015). Moreover, the expression of P25 from a PPV vector was sufficient to induce an increase in PPV pathogenicity that led to necrotic mottling in systemic leaves. Thus, systemic necrosis caused by PVX-associated synergistic infections is most probably the result of an unmitigated ER stress following the overaccumulation of a viral protein, P25, with ER remodelling activity. Another implication drawn from our results is that unidentified viral proteins with ER remodelling activities could be involved in other cases of viral synergisms, where 'helper' viruses encoding strong VSRs, such as potyviruses, exacerbate the accumulation of the partner encoding a protein with ER remodelling activity (Syller, 2012).

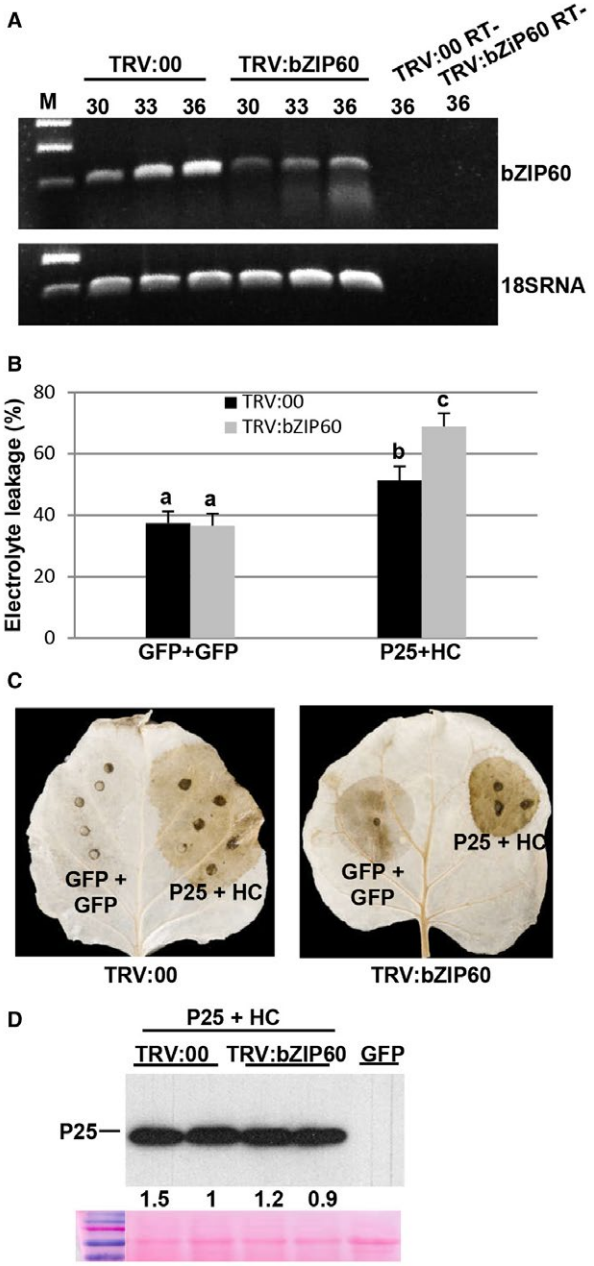

Fig. 7 Silencing of bZIP60 results in enhanced cell death induced by P25/helper component-proteinase (HC-Pro). *Nicotiana benthamiana* leaves were infiltrated with *Agrobacterium* cultures expressing pTRV2:bZIP60 or pTRV2:00 (vector control). (A) Silencing of bZIP60 transcripts was monitored by reverse transcription-polymerase chain reaction (RT-PCR) in the uppermost leaves at 20 days after inoculation (dai). The same RT reactions were used to amplify 18S RNA gene transcripts as a control. The number of PCR cycles is indicated below the treatments. RT–, control without RT. (B) At 20 dai, leaves of pTRV2:bZIP60 and control plants were agroinfiltrated with green fluorescent protein (GFP) alone or the combination of T7-tagged P25 plus HC-Pro in opposite leaf patches. Leaf discs from bZIP60-silenced and control leaves were excised and assayed for electrolyte leakage at 8 days post-infiltration (dpi). Data represent the means ± standard errors of six replicates, each consisting of four plants that received the same treatment. Statistically significant differences between means were determined by employing Scheffé's multiple range test. Different letters indicate significant differences at $P < 0.05$. (C) Leaves from bZIP60-silenced and control leaves were stained with 3,3′-diaminobenzidine (DAB) solution at 8 dpi. (D) Western blot analysis of extracts derived from leaf patches at 8 dpi, using antibodies against the T7 epitope. The lower panel below the western blot shows the Ponceau S-stained membrane after blotting, as a loading control. The intensity of the P25 bands, normalized for the loading controls, was quantified by densitometric analysis. [Colour figure can be viewed at wileyonlinelibrary.com]

Previous investigations have shown that the TGB3 protein of PVX triggers UPR and elicits PCD when expressed from TMV or under the control of the CaMV 35S promoter and delivered by agroinfiltration into *N. benthamiana* (Ye *et al.*, 2013, 2011). These findings argue that PVX encodes at least two protein products, TGB3 and P25, capable of inducing a UPR and cell death when overexpressed by either a viral vector or in the presence of a strong VSR. Although we cannot rule out a contribution of TGB3 in cell death induced by PVX-associated synergisms, we suggest that P25 is the main PVX determinant involved in the elicitation of cell death, as it has been reported that a P25 frameshift mutant clone of PVX, which maintains unaltered the TGB3 gene, does not lead to necrosis when co-expressed with VSRs (Aguilar *et al.*, 2015; this study).

BiP is an essential regulator of UPR and has been demonstrated to attenuate ER-induced cell death in several systems (Reis *et al.*, 2011; Ye *et al.*, 2013). Similarly, the overexpression of BiP contributes to alleviate the induction of cell death associated with PVX-associated synergisms. On the other hand, silencing of bZIP60 has been reported to suppress BiP transcript levels,

indicating that bZIP60 acts as an upstream signal transducer of UPR (Ye *et al.*, 2011). Thus, it was not unanticipated that overexpression of BiP and knockdown of bZIP60 would have opposite effects on the cell death caused by P25/VSR combinations. It is worth noting that the effects of overexpression of BiP and knockdown of bZIP60 on cell death caused by synergistic infection with PVX plus HC-Pro recapitulated those observed in combinations of P25 with different VSRs, indicating that the agroinfiltration assays with viral proteins recreated common mechanisms underlying PVX-associated synergisms. Moreover, it is remarkable that a significant amount of cell death was still observed in leaf patches overexpressing BiP, indicating that the pro-survival response based on BiP may be insufficient to completely inhibit cell death in PVX-associated synergisms. Indeed, previous results from our group failed to detect an alleviation of P25-induced necrosis by BiP overexpression when tissue staining to detect H_2O_2 production was used instead of the more quantitative electrolyte leakage assay (Aguilar *et al.*, 2015).

Recently, it has been reported that disruption of the host methionine cycle and the concomitant reduction in cellular glutathione levels by HC-Pro from *Potato virus A* (PVA) underlines the strong oxidative stress and the severe symptoms observed during PVX–PVA synergism in *N. benthamiana* (De *et al.*, 2018). However, we do not favour a central role of HC-Pro in the elicitation of cell death in PVX-associated synergisms, as the P25 protein, as well as PVX, induced cell death when overexpressed with VSRs derived from viruses with different biological properties, e.g. TBSV, CMV and CTV (Aguilar *et al.*, 2015; this study). Moreover, overexpression of BiP attenuated the cell death response induced by different P25/VSR combinations, suggesting a common mechanism underlying PVX-associated synergisms in *N. benthamiana*.

So far, the activation of a specific ER-dependent cell death pathway has not been documented in plants. Although it is not known precisely how P25 induces cell death, a plausible mechanism is that P25-induced membrane modification by itself or endogenous molecules exposed during P25-directed membrane rearrangement might be recognized as damage-associated molecular patterns (DAMPs), thus leading to DAMP-triggered immunity (Boller and Felix, 2009). Indeed, several studies have indicated that the modification of ER membranes attributable to the action of membrane-targeted viral proteins may be recognized as a common trigger of cell death responses against a wide range of plant viruses (Carette *et al.*, 2002; Hashimoto *et al.*, 2015; Lu *et al.*, 2016; Luan *et al.*, 2016; Ye *et al.*, 2013, 2011). The concept of DAMPs has a remarkable parallelism with the guard model for R–avr recognition (Boller and Felix, 2009), which could explain many of the similarities between P25-induced cell death and HR conferred by *R* genes (Aguilar *et al.*, 2015; García-Marcos *et al.*, 2013). For instance, SGT1 and RAR1, both of which participate in PVX/potyvirus-associated cell death, appear to positively regulate the process of cell death during non-host, effector-triggered immunity and pathogen-triggered immunity (Liu *et al.*, 2002; Wang *et al.*, 2010).

In addition to the role of UPR as a negative regulator of P25-induced cell death, overexpression of BiP restricted PVX accumulation in local tissues. Concordantly, silencing of bZIP60 increased PVX titres and virus spread to the upper parts of the plant. These data indicate that UPR partially restricts PVX infection in *N. benthamiana*, as has been reported by others at the local level using bZIP60-silenced plants (Arias Gaguancela *et al.*, 2016). However, other examples support the idea that UPR facilitates virus infection. Previous studies have shown that mutation of bZIP60 reduced the ability of TuMV to infect Arabidopsis (Zhang *et al.*, 2015). Luan *et al.* (2016) showed that the P3 protein of *Soybean mosaic virus* (SMV) targets soybean translation elongation factor 1A resulting in UPR, which, in turn, facilitates SMV replication. Such opposite observations indicate that UPR may differentially affect plant responses in distinct host–virus interactions. Nevertheless, it is noteworthy that, whereas altered accumulation of PVX in local infected leaves of bZIP60-silenced plants was dependent on the presence of HC-Pro in the inoculum, no such dependence was observed in the reduction of PVX titres mediated by BiP overexpression or in the enhanced systemic movement of the virus in bZIP60-silenced plants. The mechanisms of these effects remain unknown and need to be investigated further.

In summary, we have explored two possible mechanisms to explain the cell death induced during PVX-associated synergism in *N. benthamiana*, i.e. ER stress and elicitation of HR by the suppressor of RNA silencing protein P25 from PVX. We found no evidence that VSR activity has a causal relationship with cell death elicited by P25. Conversely, accumulation of P25 beyond a threshold level by the action of VSRs led to extensive rearrangement of ER and subsequent triggering of UPR. Failure to restore ER homeostasis ultimately led to ER collapse and cell death. Nevertheless, UPR-related gene expression still contributed to restrict PVX multiplication and spread.

EXPERIMENTAL PROCEDURES

Binary vector constructs

The PVX, PVX-GFP and PVXΔP25 binary vectors have been described previously (Aguilar *et al.*, 2015; Lu *et al.*, 2003; Peart *et al.*, 2002). The PCR amplification and cloning of T7-tagged versions of PVX P25wt or P25 mutants A104V, T117A and K124E, PPV HC-Pro, as well as PPV HCLH ($HCL_{134}H$), TBSV P19, CMV 2b, CTV P23 and the haemagglutinin (HA)-tagged *N. benthamiana* BiP genes, into *Agrobacterium tumefaciens* binary vectors has been described previously (Aguilar *et al.*, 2015). *Agrobacterium tumefaciens* carrying pCAMBIA1305.1 containing a gene encoding GUS was used

as a negative control. In some experiments, a free GFP reporter gene expressed from pCAMBIA2300 was used as a control.

The NbAGO2 ORF and NbAGO4 ORF were cloned using cDNA derived from TBSV-infected *N. benthamiana* leaves using gene-specific oligonucleotides (Table S1, see Supporting Information). The PCR products were purified and cloned into the pGEM-T easy vector (Promega, Alcobendas, Spain), and subsequently subcloned into the *Xba*I-*Bam*HI and *Xba*I-*Sma*I sites of the pBIN61 vector to yield pBIN61-NbAGO2 and pBIN61-NbAGO4, respectively. The construction of pBIN61-AtAGO2 and pBIN61-PlAMVP25 has been described previously (Brosseau and Moffett, 2015; Takeda *et al.*, 2008). Validation of overexpression of AGO mRNAs in plants was monitored by RT-PCR using gene-specific oligonucleotides (Table S1).

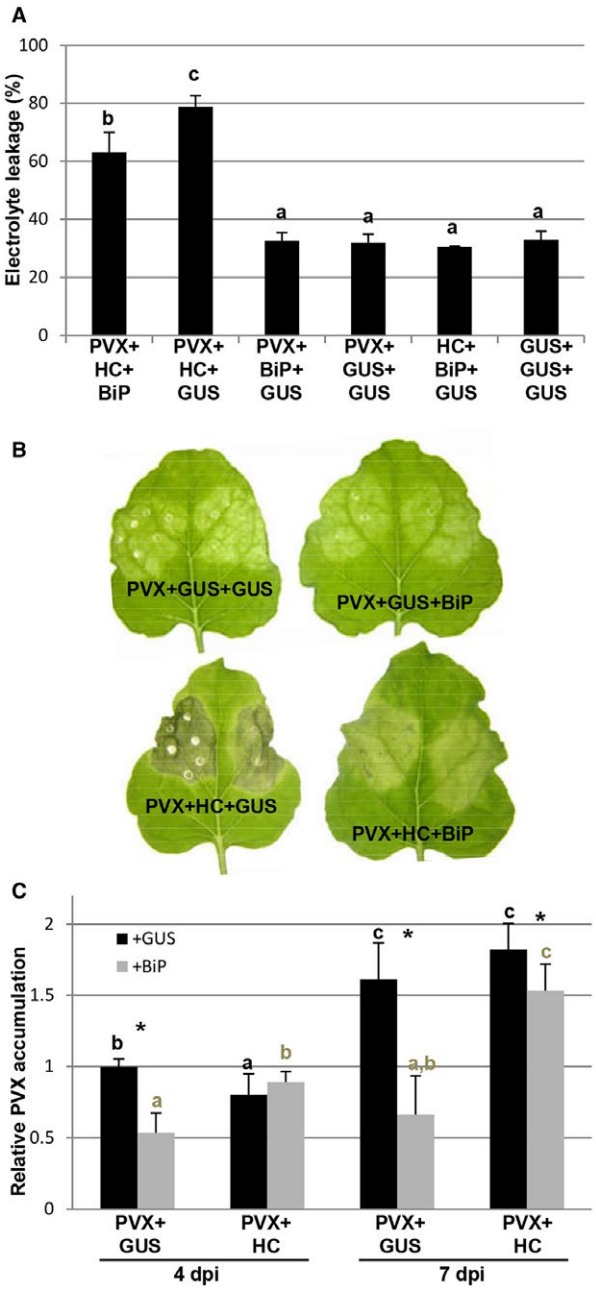

Fig. 8 The overexpression of luminal binding protein (BiP) attenuates cell death induced by *Potato virus X* (PVX) plus helper component-proteinase (HC-Pro). (A) *Nicotiana benthamiana* leaves were infiltrated with combinations of *Agrobacterium* cultures expressing PVX, HC-Pro, BiP or β-glucuronidase (GUS), as indicated. Leaf discs were excised and assayed for electrolyte leakage at 8 days post-infiltration (dpi). Data represent the means ± standard errors of 12 replicates, each consisting of four plants that received the same treatment. Statistically significant differences between means were determined by employing Scheffé's multiple range test. Different letters indicate significant differences at $P < 0.05$. (B) Representative leaves were photographed at 12 dpi. (C) Quantitative reverse transcription-polymerase chain reaction (qRT-PCR) was used to analyse the accumulation of PVX genomic RNA levels in leaf patches infected with PVX at 4 and 7 dpi. Expression of the 18S rRNA gene served as a control. Data represent the means ± standard errors of three replicates, each consisting of three plants that received the same treatment. Statistical comparisons between means were made by employing the Mann–Whitney *U*-test for between-group comparisons with a Bonferroni correction for multiple comparisons of α to $\alpha = 0.008$. Different letters indicate significant differences at $P < 0.008$. For pairwise comparisons, asterisks indicate significant differences between treatments (Mann–Whitney *U*-test, $^*P < 0.05$). [Colour figure can be viewed at wileyonlinelibrary.com]

Plant material and agroinfiltration

Nicotiana benthamiana plants, either wt or transgenic for the constitutive expression of GFP targeting the cortical ER (line 16c), were used (Ruíz *et al.*, 1998). *Nicotiana benthamiana* plants which contain hairpins to decrease endogenous DCL1, DCL2, DCL3 and DCL4 or RDR6 transcripts were described by Dadami *et al.* (2013) and Schwach *et al.* (2005), respectively. Plants were grown in a growth chamber with a 16-h light/8-h dark cycle at 25 ℃.

For transient expression assays (leaf patch assays), *A. tumefaciens* cultures were grown to exponential phase in Luria-Bertani medium with antibiotics at 28 ℃. Bacterial cultures were diluted to a final optical density of 0.6 at 600 nm. Equal volumes of each suspension were then combined and infiltration of the mixtures was performed into leaves of *N. benthamiana* plants.

Confocal microscopy

Epidermal cells in 16c *N. benthamiana*-infiltrated leaves were monitored live for fluorescence derived from GFP targeting the cortical ER at 6–8 dpi. Imaging was conducted with Leica SP2 and SP5 (Leica Microsystems GmbH, Heidelberg, Germany) confocal laser-scanning microscopes and software, using fresh leaf tissue and ×63 magnification oil immersion objectives. GFP fluorescence was excited at 488 nm and emitted light was captured at 500–530 nm.

RNA and protein gel blot analysis

Total RNA was extracted from leaf tissues as described previously (Pacheco *et al.*, 2012). qRT-PCR for the analysis of gene expression

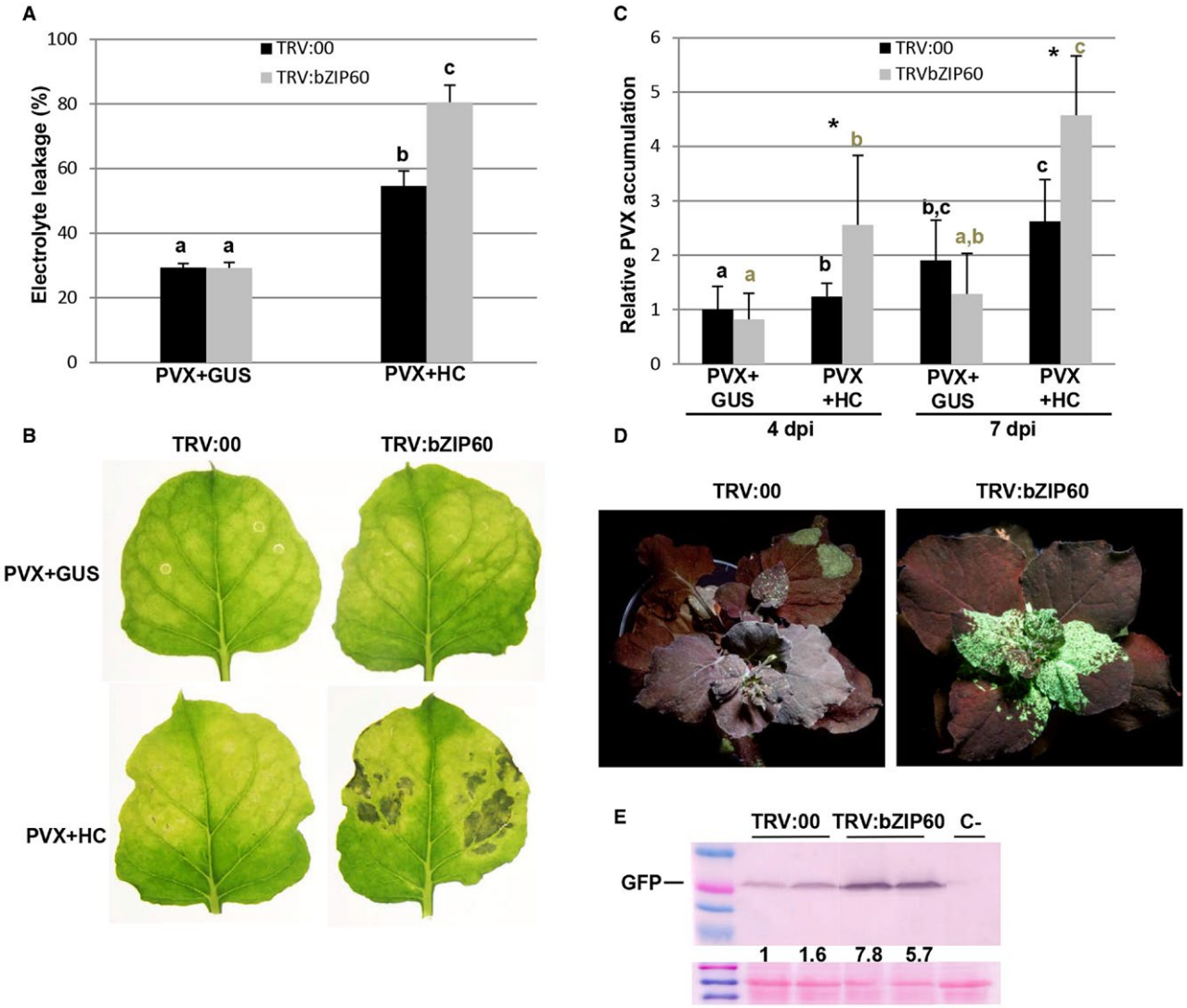

Fig. 9 Enhanced cell death in bZIP60-silenced plants infected with *Potato virus X* (PVX) plus helper component-proteinase (HC-Pro). *Nicotiana benthamiana* leaves were infiltrated with *Agrobacterium* cultures expressing pTRV2:bZIP60 or pTRV2:00 (vector control). (A) Twenty days after inoculation, leaves of pTRV2:bZIP60 and control plants were agroinfiltrated with combinations of PVX together with HC-Pro or β-glucuronidase (GUS). Leaf discs from bZIP60-silenced and control leaves were excised and assayed for electrolyte leakage at 8 days post-infiltration (dpi). Data represent the means ± standard errors of six replicates, each consisting of four plants that received the same treatment. Statistically significant differences between means were determined by employing Scheffé's multiple range test. Different letters indicate significant differences at $P < 0.05$. (B) Representative leaves were photographed at 10 dpi. (C) Quantitative reverse transcription-polymerase chain reaction (qRT-PCR) was used to analyse the accumulation of PVX genomic RNA levels in leaf patches infected with PVX at 4 and 7 dpi. Expression of the 18S rRNA gene served as a control. Data represent the means ± standard errors of six replicates, each consisting of two plants that received the same treatment. Statistical comparisons between means were made by employing Scheffé's multiple range test for between-group comparisons. Different letters indicate significant differences at $P < 0.05$. For pairwise comparisons, asterisks indicate significant differences between treatments (Student's *t*-test, $P < 0.05$). (D) bZIP60-silenced and control plants were agroinfiltrated with PVX-GFP (green fluorescent protein). Photographs were taken with long-wavelength UV light at 8 dpi. (E) Western blot analysis of extracts derived from systemic leaves at 8 dpi, using antibodies against GFP. Two independent pooled samples were analysed, each consisting of two plants that received the same treatment. The lower panel shows the Ponceau S-stained membrane after blotting, as a loading control. The intensity of the GFP bands, normalized for the loading controls, was quantified by densitometric analysis. [Colour figure can be viewed at wileyonlinelibrary.com]

was performed with gene-specific primers (Table S1). qRT-PCR for virus detection was performed using primers that amplify a region from nucleotides 2621 to 2753 of the PVX sequence, as described by García-Marcos *et al.* (2013). The relative quantification of PCR products was calculated by the comparative cycle threshold (ΔΔCt) method, as described previously (García-Marcos *et al.*, 2013). Amplification of 18S rRNA was chosen for normalization because of its similar level of expression across all treatments.

Proteins were analysed by western blot as described previously (Tena Fernández *et al.*, 2013). T7-tagged P25 was detected with horseradish peroxidase (HRP)-conjugated anti-T7 antibody (Novagen, Billerica, MA, USA) (1 : 5000 dilution). PPV HC-Pro was detected with a rabbit polyclonal antiserum (1 : 400 dilution) (González-Jara *et al.*, 2005). HA-tagged BiP was detected with a rat monoclonal antiserum to HA (Roche, Indianapolis, IN, USA) (1 : 10 000 dilution). For immunological detection of GFP, a rabbit anti-GFP, N-terminal antibody was used (Sigma-Aldrich, St. Louis, MO, USA) (1 : 3000 dilution). An appropriate secondary antibody conjugated with HRP was used in each case. Detection was performed using either the ECL system (Amersham Biosciences, Little Chalfont, UK) or with SigmaFast™ 5-bromo-4-chloro-3-indolyl-phosphate/nitro blue tetrazolium substrate tablets (Sigma-Aldrich).

Electrolyte leakage assays

The extent of cell death was measured quantitatively by monitoring electrolyte leakage. Twenty-four discs of 0.3 cm^2 were excised from the upper leaf tissue using a core borer. Discs were rinsed briefly with water and floated on 5 mL of double-distilled water for 6 h at room temperature. The conductivity of the water was measured using a conductivity meter (Crison, Barcelona, Spain). This represented the electrolyte leakage from the leaf discs (reading 1). Then, samples were boiled for 20 min at 90 ℃. After the liquid had cooled down, the conductivity of the water was measured again. This represented the total ions present in the leaf discs (reading 2). Electrolyte leakage was represented as the percentage of total ions released [(reading 1)/(reading 2) × 100]. To clarify the graphics in Fig. 4, where diverse genetic backgrounds were compared, the value of control samples was set at unity and the other data were calculated relative to this value. Reported data are means and standard errors of the values obtained in two independent experiments with 6–12 independent replicates, each consisting of pools of four plants for each treatment. Statistical analyses were performed using the statistical software IBM SPSS Statistics v.20 (IBM Corporation, Armonk, NY, USA).

For 3,3′-diaminobenzidine (DAB) staining to detect H_2O_2 production, leaves were vacuum infiltrated for 10 min with DAB solution at 1 mg/mL.

VIGS assays

A 720-bp cDNA fragment (nucleotides 435–1155) of SGS3 and a 608-bp cDNA fragment (nucleotides 168–776) of bZIP60 from *N. benthamiana* were amplified by RT-PCR using gene-specific oligonucleotides (Table S1), subsequently cut with *Bam*HI and *Xho*I, and ligated into the binary vector pTRV2 to yield pTRV2:SGS3 and pTRV2:bZIP60, respectively (Liu *et al.*, 2002). The pTRV1 vector and the pTRV2 vector and its derivatives were separately transformed into *A. tumefaciens* strain GV3101. *Nicotiana benthamiana* leaves were infiltrated with *A. tumefaciens* cultures as described above.

Silencing of RDR6 in the RDR6i transgenic line, and of SGS3 and bZIP60 in VIGS assays, was detected from upper, non-inoculated leaf tissue by RT-PCR (García-Marcos *et al.*, 2013). To ensure that similar amounts of cDNA were used for silenced and non-silenced plants, amplification of 18S rRNA or actin transcripts was employed as the internal control. Primers that anneal outside the region targeted for silencing were used to ensure that the endogenous gene would be tested (Table S1).

Drug treatment

To inhibit *de novo* lipid biosynthesis, *N. benthamiana* leaves were infiltrated with 200 μM of cerulenin (Sigma-Aldrich), which was dissolved in 2% DMSO-containing infiltration buffer for agroinfiltration.

To assess the role of the actin cytoskeleton, leaves were infiltrated with either 10 μM LatB (Merck, Danvers, MA, USA) or a DMSO buffer control at 4 days after infiltration with *Agrobacterium* cultures.

ACKNOWLEDGEMENTS

This work was supported by the Ministry of Economy and Competitiveness of Spain (grant BIO2016-75619-R [AEI/FEDER, UE]) to T.C. and F.T., and the National Science and Engineering Research Council of Canada to P.M. E.A. was a recipient of an FPU fellowship from the Spanish Ministry of Education, Culture and Sport (FPU12/01908). We thank Dr. J.A. Daròs (Instituto de Biología Molecular y Celular de Plantas, Spain) for providing *N. benthamiana* DCLi transgenic lines. We thank Dr. J.A. García (Centro Nacional de Biotecnología, Spain) for providing the *N. benthamiana* RDR6i transgenic line. There were no conflicts of interest or commercial affiliations for any authors.

REFERENCES

Aguilar, E., Almendral, D., Allende, L., Pacheco, R., Chung, B.N., Canto, T. and Tenllado, F. (2015) The P25 protein of *Potato virus X* (PVX) is the main pathogenicity determinant responsible for systemic necrosis in PVX-associated synergisms. *J. Virol.* **89**, 2090–2103.

Angel, C.A. and Schoelz, J.E. (2013) A survey of resistance to *Tomato bushy stunt virus* in the genus Nicotiana reveals that the hypersensitive response is triggered by one of three different viral proteins. *Mol. Plant–Microbe Interact.* **26**, 240–248.

Arias Gaguancela, O.P., Zúñiga, L.P., Arias, A.V., Halterman, D., Flores, F.J., Johansen, I.E., Wang, A., Yamaji, Y. and Verchot-Lubicz, J. (2016) The IRE1/bZIP60 pathway and Bax inhibitor 1 suppress systemic accumulation of potyviruses and potexviruses in *Arabidopsis* and *N. benthamiana* plants. *Mol. Plant–Microbe Interact.* **29**, 750–766.

Bao, Y. and Howell, S.H. (2017) The unfolded protein response supports plant development and defense as well as responses to abiotic stress. *Front. Plant Sci.* **8**, 1–6.

Baurès, I., Candresse, T., Leveau, A., Bendahmane, A. and Sturbois, B. (2008) The *Rx* gene confers resistance to a range of *Potexviruses* in transgenic *Nicotiana* plants. *Mol. Plant–Microbe Interact.* **21**, 1154–1164.

Boller, T. and Felix, G. (2009) A renaissance of elicitors: perception of microbe-associated molecular patterns and danger signals by pattern-recognition receptors. *Annu. Rev. Plant Biol.* **60**, 379–406.

den Boon, J.A. and Ahlquist, P. (2010) Organelle-like membrane compartmentalization of positive-strand RNA virus replication factories. *Annu. Rev. Microbiol.* **64**, 241–256.

Brosseau, C. and Moffett, P. (2015) Functional and genetic analysis identify a role for Arabidopsis ARGONAUTE5 in antiviral RNA silencing. *Plant Cell*, **27**, 1742–1754.

Carette, J.E., van Lent, J., MacFarlane, S.A., Wellink, J. and van Kammen, A. (2002) Cowpea mosaic virus 32- and 60-kilodalton replication proteins target and change the morphology of endoplasmic reticulum membranes. *J. Virol.* **76**, 6293–6301.

Chen, H.-Y., Yang, J., Lin, C. and Yuan, Y.A. (2008) Structural basis for RNA-silencing suppression by *Tomato aspermy virus* protein 2b. *EMBO Rep.* **9**, 754–760.

Chiu, M.H., Chen, I.H., Baulcombe, D.C. and Tsai, C.H. (2010) The silencing suppressor P25 of *Potato virus X* interacts with Argonaute1 and mediates its degradation through the proteasome pathway. *Mol. Plant Pathol.* **11**, 641–649.

Dadami, E., Boutla, A., Vrettos, N., Tzortzakaki, S., Karakasilioti, I. and Kalantidis, K. (2013) DICER-LIKE 4 but not DICER-LIKE 2 may have a positive effect on potato spindle tuber viroid accumulation in *Nicotiana benthamiana*. *Mol. Plant*, **6**, 232–234.

De, S., Chavez-Calvillo, G., Wahlsten, M. and Mäkinen, K. (2018) Disruption of the methionine cycle and reduced cellular gluthathione levels underlie *potex-potyvirus* synergism in Nicotiana benthamiana. *Mol. Plant Pathol.* **19**, 1820–1835.

García-Marcos, A., Pacheco, R., Manzano, A., Aguilar, E. and Tenllado, F. (2013) Oxylipin biosynthesis genes positively regulate programmed cell death during compatible infections with the synergistic pair *Potato virus X–Potato virus Y* and *Tomato spotted wilt virus*. *J. Virol.* **87**, 5769–5783.

García-Marcos, A., Pacheco, R., Martiáñez, J., González-Jara, P., Díaz-Ruíz, J.R. and Tenllado, F. (2009) Transcriptional changes and oxidative stress associated with the synergistic interaction between *Potato virus X* and *Potato virus Y* and their relationship with symptom expression. *Mol. Plant–Microbe Interact.* **22**, 1431–1444.

González-Jara, P., Atencio, F.A., Martínez-García, B., Barajas, D., Tenllado, F. and Díaz-Ruíz, J.R. (2005) A single amino acid mutation in the Plum pox virus helper component-proteinase gene abolishes both synergistic and RNA silencing suppression activities. *Phytopathology*, **95**, 894–901.

González-Jara, P., Tenllado, F., Martínez-García, B., Atencio, F.A., Barajas, D., Vargas, M., Díaz-Ruíz, J. and Díaz-Ruíz, J.R. (2004) Host-dependent differences during synergistic infection by potyviruses with Potato virus X. *Mol. Plant Pathol.* **5**, 29–35.

Hashimoto, M., Komatsu, K., Iwai, R., Keima, T., Maejima, K., Shiraishi, T., Ishikawa, K., Yoshida, T., Kitazawa, Y., Okano, Y. and Yamaji, Y. (2015) Cell death triggered by a putative amphipathic helix of *Radish mosaic virus* helicase protein is tightly correlated with host membrane modification. *Mol. Plant–Microbe Interact.* **28**, 675–688.

Király, L., Cole, A.B., Bourque, J.E. and Schoelz, J.E. (1999) Systemic cell death is elicited by the interaction of a single gene in *Nicotiana clevelandii* and gene VI of Cauliflower mosaic virus. *Mol. Plant–Microbe Interact.* **12**, 919–925.

Komatsu, K., Hashimoto, M., Ozeki, J., Yamaji, Y., Maejima, K., Senshu, H., Himeno, M., Okano, Y., Kagiwada, S. and Namba, S. (2010) Viral-induced systemic necrosis in plants involves both programmed cell death and the inhibition of viral multiplication, which are regulated by independent pathways. *Mol. Plant–Microbe Interact.* **23**, 283–293.

Li, H.W., Lucy, A.P., Guo, H.S., Li, W.X., Ji, L.H., Wong, S.M. and Ding, S.W. (1999) Strong host resistance targeted against a viral suppressor of the plant gene silencing defence mechanism. *EMBO J.* **18**, 2683–2691.

Liu, Y.L., Schiff, M., Marathe, R. and Dinesh-Kumar, S.P. (2002) Tobacco Rar1, EDS1 and NPR1/NIM1 like genes are required for N-mediated resistance to tobacco mosaic virus. *Plant J.* **30**, 415–429.

Lu, R., Malcuit, I., Moffett, P., Ruiz, M.T., Peart, J., Wu, A.J., Rathjen, J.P., Bendahmane, A., Day, L. and Baulcombe, D.C. (2003) High throughput virus-induced gene silencing implicates heat shock protein 90 in plant disease resistance. *EMBO J.* **22**, 5690–5699.

Lu, Y., Yin, M., Wang, X., Chen, B., Yang, X., Peng, J., Zheng, H., Zhao, J., Lin, L., Yu, C. and MacFarlane, S. (2016) The unfolded protein response and programmed cell death are induced by expression of Garlic virus X p11 in *Nicotiana benthamiana*. *J. Gen. Virol.* **97**, 1462–1468.

Luan, H., Shine, M.B., Cui, X., Chen, X., Ma, N., Kachroo, P., Zhi, H. and Kachroo, A. (2016) The potyviral P3 protein targets eukaryotic elongation factor 1A to promote the unfolded protein response and viral pathogenesis. *Plant Physiol.* **172**, 221–234.

Mackey, D., Holt, B.F., Wiig, A. and Dangl, J.L. (2002) RIN4 interacts with *Pseudomonas syringae* type III effector molecules and is required for RPM1-mediated resistance in *Arabidopsis*. *Cell*, **108**, 743–754.

Malcuit, I., Marano, M.R., Kavanagh, T.A., De Jong, W., Forsyth, A. and Baulcombe, D.C. (1999) The 25-kDa movement protein of PVX elicits *Nb*-mediated hypersensitive cell death in potato. *Mol. Plant–Microbe Interact.* **12**, 536–543.

Mandadi, K.K. and Scholthof, K.-B.G. (2013) Plant immune responses against viruses: how does a virus cause disease? *Plant Cell*, **25**, 1489–1505.

Moffett, P. (2016) Using decoys to detect pathogens: an integrated approach. *Trends Plant Sci.* **21**, 369–370.

Okano, Y., Senshu, H., Hashimoto, M., Neriya, Y., Netsu, O., Minato, N., Yoshida, T., Maejima, K., Oshima, K., Komatsu, K., Yamaji, Y. and Namba, S. (2014) In planta recognition of a double-stranded RNA synthesis protein complex by a potexviral RNA silencing suppressor. *Plant Cell*, **26**, 2168–2183.

Omura, S. (1976) The antibiotic cerulenin, a novel tool for biochemistry as an inhibitor of fatty acid synthesis. *Bacteriol. Rev.* **40**, 681–697.

Pacheco, R., García-Marcos, A., Manzano, A., de Lacoba, M.G., Camañes, G., García-Agustín, P., Díaz-Ruíz, J.R. and Tenllado, F. (2012) Comparative analysis of transcriptomic and hormonal responses to compatible and incompatible plant–virus interactions that lead to cell death. *Mol. Plant–Microbe Interact.* **25**, 709–723.

Peart, J.R., Cook, G., Feys, B.J., Parker, J.E., Baulcombe, D.C., Centre, J.I., Lane, C. and Nr, N. (2002) An EDS1 orthologue is required for N-mediated resistance against tobacco mosaic virus. *Plant J.* **29**, 569–579.

Reis, P.A.A., Rosado, G.I., Silva, L.A.C., Oliveira, L.C., Oliveira, L.B., Costa, M.D.L., Alvim, F.C. and Fontes, E.P.B. (2011) The binding protein BiP attenuates stress-induced cell death in soybean via modulation of the N-rich protein-mediated signaling pathway. *Plant Physiol.* **157**, 1853–1865.

de Ronde, D., Pasquier, A., Ying, S., Butterbach, P., Lohuis, D. and Kormelink, R. (2014) Analysis of *Tomato spotted wilt virus* NSs protein indicates the importance of the N-terminal domain for avirulence and RNA silencing suppression. *Mol. Plant Pathol.* **15**, 185–195.

Ruíz, M.T., Voinnet, O. and Baulcombe, D.C. (1998) Initiation and maintenance of virus-induced gene silencing. *Plant Cell*, **10**, 937–946.

Schwach, F., Vaistij, F.E., Jones, L. and Baulcombe, D.C. (2005) An RNA-dependent RNA polymerase prevents meristem invasion by Potato virus X and is required for the activity but not the production of a systemic silencing signal. *Plant Physiol.* **138**, 1842–1852.

Senshu, H., Ozeki, J., Komatsu, K., Hashimoto, M., Hatada, K., Aoyama, M., Kagiwada, S., Yamaji, Y. and Namba, S. (2009) Variability in the level of RNA silencing suppression caused by triple gene block protein 1 (TGBp1) from various potexviruses during infection. *J. Gen. Virol.* **90**, 1014–1024.

Sparkes, I.A., Frigerio, L., Tolley, N. and Hawes, C. (2009) The plant endoplasmic reticulum: a cell-wide web. *Biochem. J.* **423**, 145–155.

Sun, Z., Yang, D., Xie, L., Sun, L., Zhang, S., Zhu, Q., Li, J., Wang, X. and Chen, J. (2013) *Rice black-streaked dwarf virus* P10 induces membranous structures at the ER and elicits the unfolded protein response in *Nicotiana benthamiana*. *Virology*, **447**, 131–139.

Syller, J. (2012) Facilitative and antagonistic interactions between plant viruses in mixed infections. *Mol. Plant Pathol.* **13**, 204–216.

Takeda, A., Iwasaki, S., Watanabe, T., Utsumi, M. and Watanabe, Y. (2008) The mechanism selecting the guide strand from small RNA duplexes is different among Argonaute proteins. *Plant Cell Physiol.* **49**, 493–500.

Tena Fernández, F., González, I., Doblas, P., Rodríguez, C., Sahana, N., Kaur, H., Tenllado, F., Praveen, S. and Canto, T. (2013) The influence of cis-acting P1 protein and translational elements on the expression of *Potato virus Y* helper-component proteinase (HCPro) in heterologous systems and its suppression of silencing activity. *Mol. Plant Pathol.* **14**, 530–541.

Tilsner, J., Linnik, O., Wright, K.M., Bell, K., Roberts, A.G., Lacomme, C., Santa Cruz, S. and Oparka, K.J. (2012) The TGB1 movement protein of *Potato virus X* reorganizes actin and endomembranes into the X-Body, a viral replication factory. *Plant Physiol.* **158**, 1359–1370.

Vance, V.B. (1991) Replication of Potato virus X RNA is altered in coinfections with Potato virus Y. *Virology*, **182**, 486–494.

Verchot, J., Angell, S.M. and Baulcombe, D.C. (1998) In vivo translation of the triple gene block of potato virus X requires two subgenomic mRNAs. *J. Virol.* **72**, 8316–8320.

Wang, K., Empleo, R., Nguyen, T.T.V., Moffett, P. and Sacco, M.A. (2015) Elicitation of hypersensitive responses in *Nicotiana glutinosa* by the suppressor of RNA silencing protein P0 from poleroviruses. *Mol. Plant Pathol.* **16**, 435–448.

Wang, K., Uppalapati, S.R., Zhu, X., Dinesh-Kumar, S.P. and Mysore, K.S. (2010) SGT1 positively regulates the process of plant cell death during both compatible and incompatible plant–pathogen interactions. *Mol. Plant Pathol.* **11**, 597–611.

Williams, B., Verchot, J. and Dickman, M.B. (2014) When supply does not meet demand—ER stress and plant programmed cell death. *Front. Plant Sci.* **5**, 1–9.

Ye, C.M., Chen, S., Payton, M., Dickman, M.B. and Verchot, J. (2013) TGBp3 triggers the unfolded protein response and SKP1-dependent programmed cell death. *Mol. Plant Pathol.* **14**, 241–255.

Ye, C.M., Dickman, M.B., Whitham, S.A., Payton, M. and Verchot, J. (2011) The unfolded protein response is triggered by a plant viral movement protein. *Plant Physiol.* **156**, 741–755.

Zhang, L., Chen, H., Brandizzi, F., Verchot, J. and Wang, A. (2015) The UPR branch IRE1-bZIP60 in plants plays an essential role in viral infection and is complementary to the only UPR pathway in yeast. *PLoS Genet.* **11**, 1–37.

SUPPORTING INFORMATION

Additional supporting information may be found in the online version of this article at the publisher's web site:

Fig. S1 Expression of PVX P25 together with PPV HC-Pro elicits cell death in *N. benthamiana*. (A) Leaf was infiltrated with combinations of *Agrobacterium* cultures expressing PVX plus either HC-Pro, HCLH or GFP, and expressing HC-Pro plus GFP, as indicated. (B) Leaf was infiltrated with combinations of *Agrobacterium* cultures expressing PVX P25 plus either HC-Pro, HCLH, or GFP, and expressing HC-Pro plus GFP, as indicated. (C) Leaf was infiltrated with combinations of *Agrobacterium* cultures expressing HC-Pro plus either PVX or PVXΔP25. Leaves were photographed at 10 days post-infiltration. HCLH is a variant of PPV HC-Pro containing a single point mutation ($L_{134}H$) and is unable to induce the systemic necrosis response when expressed from a PVX vector (González-Jara *et al.*, 2005).

Fig. S2 Validation of silencing of RNA silencing components and AGO overexpression in *N. benthamiana* plants. (A) Silencing of RDR6 transcripts was monitored by RT-PCR in RDR6i transgenic line. (B) Silencing of SGS3 transcripts was monitored by RT-PCR in uppermost leaves at 20 days after inoculation with pTRV2:SGS3 or pTRV2:00 (vector control). The same RT reactions were used to amplify actin transcripts as a control. The number of PCR cycles is indicated below treatments. (C) Overexpression of NbAGO2 (upper panels), NbAGO4 (middle panels) and AtAGO2 (bottom panels) transcripts was monitored by RT-PCR at 5 days after infiltration with the respective constructs.

Fig. S3 BiP overexpression attenuated the cell death response in leaves infiltrated with P25 together with suppressors of RNA silencing. Leaves of *N. benthamiana* were infiltrated with combinations of *Agrobacterium* cultures expressing PVX P25 plus either PPV HC-Pro, TBSV P19, CMV 2b, or CTV P23 and expressing PlAMV P25 plus HC-Pro in combination with either GFP or BiP, as indicated. Leaves were stained with DAB solution at 8 days post-infiltration.

Fig. S4 qRT-PCR was used to analyze the accumulation of PVX genomic RNA levels in leaf patches infiltrated with PVX plus either HC-Pro, BiP or GUS at 3 and 6 days post-infiltration (dpi). Expression of the 18S rRNA gene served as a control. Data represent the means ± standard errors of 3 replicates, each consisting of three plants that received the same treatment. Statistical comparisons between means were made by employing Mann-Whitney U test for between-groups comparisons with a Bonferroni correction for multiple comparisons of α to $\alpha = 0.008$. Different letters indicate significant differences at $P < 0.008$. For pairwise comparisons, asterisks indicate significantdifferences between treatments (Mann-Whitney U test, * $P < 0.05$).

Table S1 Primers used for RT-PCRs and construction of clones.